Augmented TLR9-induced Btk activation in PIR-B–deficient B-1 cells provokes excessive autoantibody production and autoimmunity

Tomohiro Kubo,[1,2] Yuki Uchida,[1] Yuko Watanabe,[1] Masahiro Abe,[1] Akira Nakamura,[1] Masao Ono,[3] Shizuo Akira,[4] and Toshiyuki Takai[1]

[1]Department of Experimental Immunology, Institute of Development, Aging, and Cancer, Tohoku University, Sendai 980-8575, Japan
[2]Department of Pediatrics, Self Defense Force Sendai Hospital, Sendai 983-0041, Japan
[3]Department of Pathology, Tohoku University Graduate School of Medicine, Sendai 980-8575, Japan
[4]Laboratory of Host Defense, World Premiere International Immunology Frontier Research Center, Osaka University, Suita, Osaka 565-0871, Japan

Pathogens are sensed by Toll-like receptors (TLRs) expressed in leukocytes in the innate immune system. However, excess stimulation of TLR pathways is supposed to be connected with provocation of autoimmunity. We show that paired immunoglobulin (Ig)-like receptor B (PIR-B), an immunoreceptor tyrosine-based inhibitory motif–harboring receptor for major histocompatibility class I molecules, on relatively primitive B cells, B-1 cells, suppresses TLR9 signaling via Bruton's tyrosine kinase (Btk) dephosphorylation, which leads to attenuated activation of nuclear factor κB p65RelA but not p38 or Erk, and blocks the production of natural IgM antibodies, including anti-IgG Fc autoantibodies, particularly rheumatoid factor. The autoantibody production in PIR-B–deficient (*Pirb*$^{-/-}$) mice was further augmented in combination with the *Fas*^{lpr} mutation, which might be linked to the development of autoimmune glomerulonephritis. These results show the critical link between TLR9-mediated sensing and a simultaneously evoked, PIR-B–mediated inhibitory circuit with a Btk intersection in B-1 cells, and suggest a novel way toward preventing pathogenic natural autoantibody production.

CORRESPONDENCE
Toshiyuki Takai:
tostakai@idac.tohoku.ac.jp

Abbreviations used: β2-GPI, β2–glycoprotein I; Btk, Bruton's tyrosine kinase; ds, double stranded; HRP, horseradish peroxidase; ITIM, immunoreceptor tyrosine-based inhibitory motif; MAPK, mitogen-activated protein kinase; PAS, periodic acid–Schiff; PIR-B, paired Ig-like receptor B; PVDF, polyvinylidene difluoride; RF, rheumatoid factor; SHP-1, SH2 domain–containing tyrosine phosphatase 1; ss, single stranded; TLR, Toll-like receptor.

The emergence of autoimmunity is often coupled with aging, and is suggested to be linked to activation of the innate immune system in individuals suffering from bacterial and viral infections (Baccala et al., 2007; Groom et al., 2007; Krieg and Vollmer 2007; Rothlin et al., 2007). Toll-like receptors (TLRs) expressed in leukocytes of the innate immune system play indispensable roles in the sensing of viral and bacterial invasion through binding pathogen-associated molecular patterns, which leads to efficient T cell–mediated inflammatory responses (Akira et al., 2001; Iwasaki and Medzhitov, 2004). The TLR-mediated priming of inflammation and production of neutralizing antibodies against pathogens should be strictly regulated, otherwise there is the possibility of the development of autoimmune diseases (Marsland and Kopf, 2007). The mechanisms underlying the efficient TLR-mediated activation of the innate and adaptive immune systems with prevention of reactivity to autologous tissues remain elusive.

Examples of critical cells that express TLRs and could potentially link the innate and adaptive immune systems are relatively primitive B cells, B-1 cells, found mainly in the peritoneal and pleural cavities. In contrast to recirculating follicular B cells (or conventional B or B-2 cells), B-1 cells are characterized by $B220^{low}IgM^{high}CD23^{-}CD43^{+}IgD^{low}$ cells (Berland and Wortis, 2002; Tung and Herzenberg, 2007). Although it has been pointed out by many researchers that innate B-1 cells but not conventional B cells are producers of natural antibodies against pathogens (Ochsenbein et al., 1999), accumulating lines of evidence suggest that a major source of autoantibodies is also those B-1 cells (Baumgarth et al., 2005; Carroll and Holers, 2005), but it has been a matter of debate.

The Rockefeller University Press $30.00
J. Exp. Med. Vol. 206 No. 9 1971-1982
www.jem.org/cgi/doi/10.1084/jem.20082392

The Journal of Experimental Medicine

By stimulation via different TLRs, the B-1 cell population in the peritoneal cavity has been enlarged and B-1 cell–mediated autoantibody production augmented (Murakami et al., 1995). This could be partly because B-1 cells express a set of TLRs, including TLR4, TLR7, and TLR9 (Gururajan et al., 2007), and are more prone to differentiate into plasma cells than B-2 cells upon TLR-mediated stimulation, although B-2 cells similarly possess a range of TLRs (Genestier et al., 2007). For example, Murakami et al. (1995) have shown, in anti–red blood cell autoantibody transgenic mice, that the susceptibility to autoimmune hemolytic anemia was significantly increased when the mice were transferred from germ-free or specific pathogen-free conditions to conventional conditions or injected with a TLR4 ligand, LPS, with a concomitant increase in the peritoneal B-1 cell population, whereas almost all B-2 cells are constitutively deleted in the transgenic mice. These findings again suggest the importance of the regulation of TLR signaling in B-1 cells, which prevents overstimulation of TLRs so as not to evoke overproduction of natural antibodies, including potentially harmful autoantibodies. Therefore, what mechanisms may regulate the overstimulation of the TLR signal, particularly in B-1 cells?

We speculated that paired Ig-like receptor B (PIR-B; Hayami et al., 1997; Kubagawa et al., 1997) could participate in the regulation of B-1 cells. Recruitment of SH2 domain–containing tyrosine phosphatase 1 (SHP-1) to phosphotyrosylated immunoreceptor tyrosine-based inhibitory motifs (ITIMs) in the cytoplasmic portion of PIR-B was shown to be critical for PIR-B–mediated inhibitory signaling in general (Ho et al., 1999; Maeda et al., 1999), and this inhibition is achieved, at least in part, via constitutive binding of PIR-B to its ligand, i.e., MHC class I molecules, expressed on the same cell surface (Masuda et al., 2007). Interestingly, in PIR-B–deficient (*Pirb*$^{-/-}$) mice, the peritoneal B-1 cell population significantly increased, particularly with aging, compared with wild-type mice (Ujike et al., 2002). However, it has not been determined how the B-1 cell compartment is physiologically regulated by PIR-B or what the physiological or pathological consequence of the expanded B-1 cells is in the contexts of infection and autoimmunity.

In this paper, we show that PIR-B can inhibit TLR9-mediated signaling via regulation of Bruton's tyrosine kinase (Btk) phosphorylation in peritoneal B-1 cells. We found that TLR9 activation immediately activates an Src family kinase, Lyn, which then phosphorylates PIR-B cytoplasmic ITIMs. In the absence of PIR-B, B-1 cells become hyperproducers of natural IgM antibodies, including anti-IgG Fc autoantibodies, i.e., rheumatoid factor (RF), via unmethylated CpG-B oligodeoxynucleotide (CpG-B) stimulation in vitro and in vivo or upon aging. These phenotypes caused by PIR-B deficiency were further exaggerated in combination with the *Fas*^{lpr} mutation, which caused the *Pirb*$^{-/-}$*Fas*^{lpr} mutant mice to be short-lived mainly because of autoimmune glomerulonephritis with immune complex depositions. Our findings may provide a novel strategy for preventing autoimmunity by reducing the production of pathogenic autoantibodies by B-1 cells, such as through down-regulation of Btk activation or enhancement of PIR-B–mediated B-1 cell regulation.

RESULTS

PIR-B deficiency with *Fas*^{lpr} mutation characteristically augments autoantibody production associated with autoimmune glomerulonephritis

Pirb$^{-/-}$ mice were grossly normal and survived well to at least 50 wk of age (Fig. 1 A) without any abnormalities in the histology of their joint components (synovium and cartilage; Fig. S1 A), skin, lungs, and glomeruli (not depicted). However, *Pirb*$^{-/-}$*Fas*^{lpr} mice were found to be markedly short-lived, with only about half of them surviving at 40 wk of age (Fig. 1 A). Microscopic examination of their organ samples revealed that the combined mutant mice did not develop histopathological traits in the lung, salivary glands (not depicted), and joints (Fig. S1 A), but that in the kidney they readily developed diffuse glomerulopathy with a mild increase in the size and cellularity (mesangial area) of the glomerulus (Fig. 1 B, periodic acid–Schiff [PAS] stain). Immunofluorescence analysis revealed substantial deposition of IgG, IgM, and C3 in *Pirb*$^{-/-}$*Fas*^{lpr} mice (Fig. 1 B). These pathological changes were not observed in wild-type B6 or *Fas*^{lpr} mice, indicating that autoimmune glomerulonephritis occurs as a combined effect of PIR-B and Fas mutations (Fig. S1 B). Consistent with no arthritis and Sjögren-like disease in the double-mutant mice, anti–SS-B/La antibodies were below the detection limit (Fig. S1 C, left). We also found that, although the levels of IgM- and IgG-RF were high in *Fas*^{lpr} mice, these levels were further elevated in *Pirb*$^{-/-}$*Fas*^{lpr} mice (Fig. 1 C), indicating that PIR-B deficiency has a marked impact on the augmentation of RF production in vivo. In addition, anti–double-stranded (ds) DNA autoantibody production was more augmented in *Pirb*$^{-/-}$*Fas*^{lpr} mice than in *Fas*^{lpr} animals, although the difference did not reach a statistically significant level (Fig. 1 D). We also measured by ELISA the levels of autoantibodies in sera against single-stranded (ss) DNA and β2–glycoprotein I (β2-GPI), but we did not observe a significant elevation of anti-ssDNA production in *Pirb*$^{-/-}$*Fas*^{lpr} mice tested compared with *Fas*^{lpr} animals (Fig. 1 D, right), nor we did not detect anti–β2-GPI (Fig. S1 C, right). Examinations of hematocrit values failed to demonstrate an autoimmune hemolytic anemia in *Pirb*$^{-/-}$*Fas*^{lpr} and other mice (Table S1). The PIR-B deficiency did not result in any obvious changes in the staining pattern by antinuclear autoantibodies (Fig. S1 D). The peritoneal B-1 cell (Fig. 1 E, top) and splenic plasma cell (Fig. 1 E, bottom) populations were also markedly increased in *Pirb*$^{-/-}$*Fas*^{lpr} mice. With these data collectively, we concluded that PIR-B deficiency renders mice susceptible to the development of autoimmune glomerulonephritis in combination with *Fas*^{lpr}, which accompanies with a markedly elevated RF production, with a robust production of anti-dsDNA and anti-ssDNA autoantibodies.

Elevated RF production in *Pirb*$^{-/-}$ mice administered with CpG-B DNA

RF is one of the autoreactive natural antibodies whose primary role is believed to be the first-line defense against infection.

The main source of such autoantibodies is considered to be B-1 cells (Montecino-Rodriguez and Dorshkind, 2006). Adequate regulation of the production of natural autoantibodies, including RF, is proposed to be crucial for avoiding autoimmune diseases, which are otherwise evoked by too strong or sustained innate responses against microbial or viral infections (Murakami et al., 1995; Akira et al., 2001; De Re et al., 2006; Krieg and Vollmer, 2007; Marsland and Kopf, 2007). To

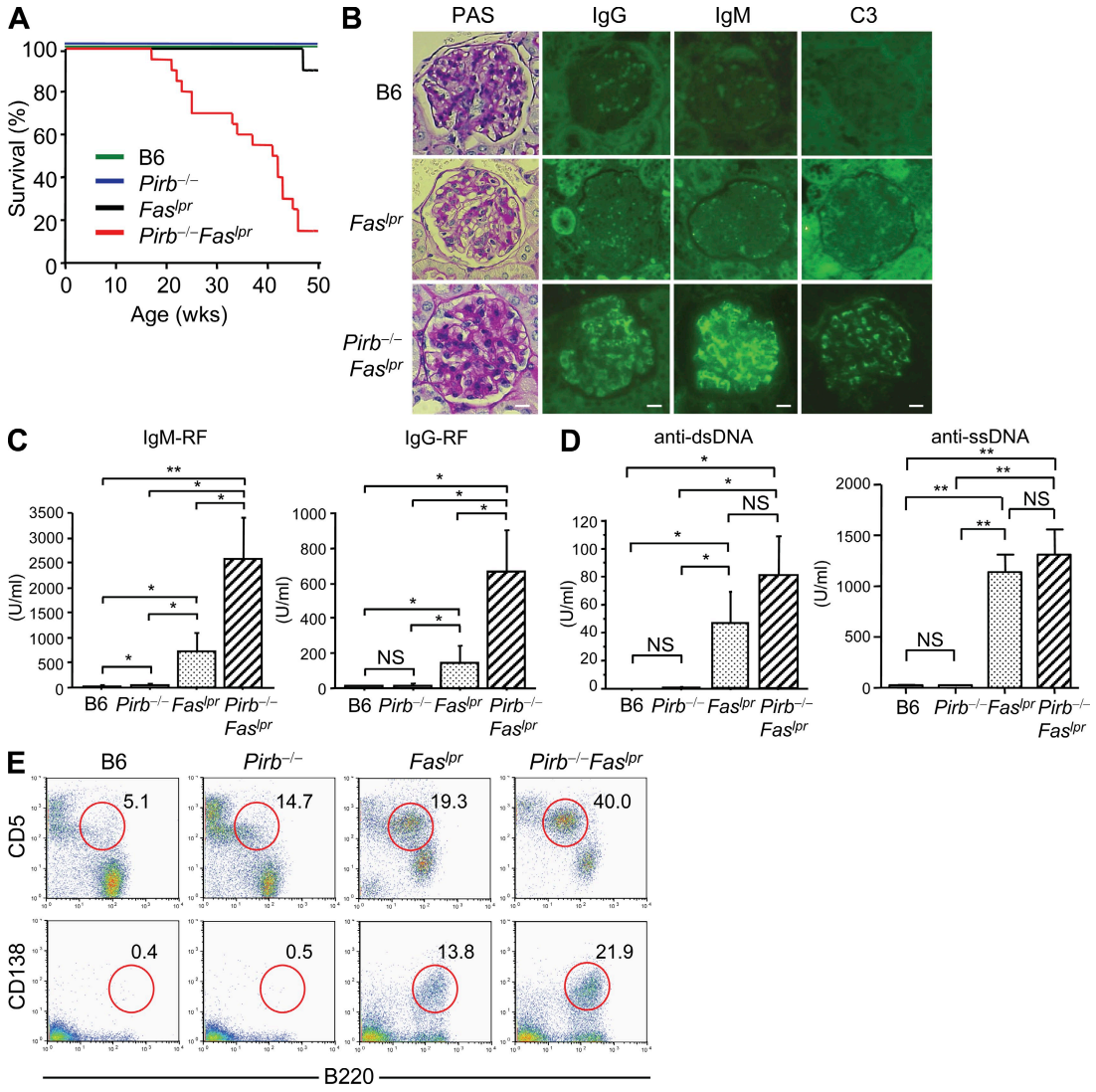

Figure 1. *Pirb*$^{-/-}$ with the *Fas*^{lpr} mutation is sufficient in mice for the development of glomerulonephritis with marked elevation of RF production. (A) *Pirb*$^{-/-}$*Fas*^{lpr} mice were remarkably short-lived. The survival curves for male and female B6.*Pirb*$^{-/-}$*Fas*^{lpr} (n = 20 mice per group), B6.*Fas*^{lpr} (n = 20), B6.*Pirb*$^{-/-}$ (n = 20), and B6 (n = 20) mice until 50 wk of age are shown. (B) *Pirb*$^{-/-}$*Fas*^{lpr} mice develop diffuse glomerulonephritis with a mild increase in the size and cellularity of the glomerulus, and depositions of IgG, IgM, and complement C3. Kidney sections from each strain of mice at 24 wk of age were stained with PAS or Alexa Fluor 488 anti-mouse IgG, IgM, and C3. Each panel is representative of samples from five mice per group with similar staining profiles in a single staining experiment. Bars, 10 µm. (C) Both the IgM- and IgG-RF levels were significantly more elevated in *Pirb*$^{-/-}$*Fas*^{lpr} mice than those in *Fas*^{lpr} mice. RF in sera from each strain of mice at 24 wk of age was measured by ELISA. Data are shown as means ± SEM (n = 8 mice per group) and are representative of three separate experiments with similar results. Statistical analyses were performed using a Student's t test. *, $P < 0.05$; **, $P < 0.01$. (D) The anti-dsDNA and anti-ssDNA autoantibody levels were augmented but not significantly elevated in the *Pirb*$^{-/-}$*Fas*^{lpr} mice tested compared with *Fas*^{lpr} mice. Anti-DNA in sera from each strain of mice at 24 wk of age for anti-dsDNA or at 4–10 mo of age for anti-ssDNA was measured by ELISA. Data are shown as means ± SEM (n = 8 mice per group) and are representative of three (anti-dsDNA) or two (anti-ssDNA) separate experiments with similar results. Statistical analyses were performed using a Student's t test. *, $P < 0.05$; **, $P < 0.01$. (E) Markedly enlarged peritoneal B-1 cell and splenic plasma cell populations in *Pirb*$^{-/-}$*Fas*^{lpr} mice. Peritoneal cells isolated from 24-wk-old mice were stained with anti-B220, CD5, and CD3. B220^{+}CD5^{+}CD3^{-} B-1 cells (circled) with the percentages are shown (top). Staining of peritoneal cells from *Pirb*$^{-/-}$ mice with anti-CD19, instead of B220, gave a B-1 cell population with a similar size (not depicted in the figure). Splenocytes isolated from 24-wk-old mice were stained with anti-CD138, B220, IgM, and IgD. CD138^{+}B220^{+}IgM^{-}IgD^{-} plasma cells (circled) with the percentages are shown (bottom). The figure is representative of five mice per group.

characterize the precise sources of RF, we next examined the RF levels in sera from B6 and *Pirb*$^{-/-}$ mice in the absence of a potentially large influence by *Fas*^{lpr} mutation. Although 8- and 40-wk-old B6 wild-type mice did not show notable production of either IgM-RF or IgG-RF, *Pirb*$^{-/-}$ mice at 40 wk of age exhibited significantly higher levels of IgM-RF and slightly elevated IgG-RF levels (Fig. 2 A). When we intraperitoneally injected 3 nmol CpG-B DNA, a ligand for TLR9, into 8-wk-old B6 and *Pirb*$^{-/-}$ mice, and determined IgM-RF and IgG-RF levels in their sera after 48 and 120 h, respectively, we found that the RF of both classes was significantly elevated in *Pirb*$^{-/-}$ but not in B6 mice (Fig. 2 B), suggesting that CpG-B–responsive cells in the peritoneal cavity produce RF. Diminishing B-1 cells, as well as B-2 cells, in the peritoneum by repeated injection of water (Fig. S2; Murakami et al., 1995) resulted in a significant reduction of the total IgM level and a nearly complete abrogation of IgM-RF production in *Pirb*$^{-/-}$ mice comparable to that in wild-type mice (Fig. 2 C). These results suggest that peritoneal B cells are a major source of IgM-RF autoantibodies in *Pirb*$^{-/-}$ mice.

Augmented CpG-B responses in PIR-B–deficient B-1 cells in vitro

Next, we aimed at examining more precisely the PIR-B–mediated regulation of RF production by B-1 cells in vitro. We sorted B220^{+}CD11b^{+} B-1 cells from peritoneal cells of B6 and *Pirb*$^{-/-}$ mice, and examined them for their proliferation upon stimulation with various TLR ligands. B-1 cells from both B6 and *Pirb*$^{-/-}$ mice were found to respond well to LPS (TLR4 ligand) and CpG-B (TLR9 ligand), but not to poly(I:C) (TLR3 ligand) or ssRNA (TLR7/8 ligand; Fig. 3 A), indicating the significant roles of TLR4 and TLR9 in the B-1 cell function, as pointed out previously (Gururajan et al., 2007). Interestingly, however, stimulation of *Pirb*$^{-/-}$ B-1 cells with CpG-B provoked higher proliferation than that of wild-type cells, whereas the LPS-mediated responses were comparable. The CpG-B–mediated augmented proliferation seen for *Pirb*$^{-/-}$ B-1 cells was not observed for splenic B-2 cells (Fig. 3 B, left), as in the case of LPS (Fig. 3 B, right). These results indicate that *Pirb*$^{-/-}$ peritoneal B-1 cells, but not the splenic B-2 cells, were more sensitive to CpG-B stimulation and divided more vigorously than those from wild-type mice. We observed that B-1 cells express about sixfold more PIR-B molecules on their surface than splenic B-2 cells, whereas the TLR9 expression levels are comparable between B-1 and B-2 cells when estimated by flow cytometry (Fig. S2, A and B). We also noted that the expression level of Btk, one of the signal mediators downstream of PIR-B (Maeda et al., 1999), is higher in B-1 cells than that in B-2 cells (Fig. S3, C and D). These observations may account for, at least partly, the difference in the sensitivity to CpG-B between B-1 and B-2 cells.

This observation of CpG-B–sensitive *Pirb*$^{-/-}$ B-1 cells prompted us to examine whether other possible B-1 cell products (Baumgarth et al., 2005; Carroll and Holers, 2005; Gururajan et al., 2007) could also be elevated. A culture

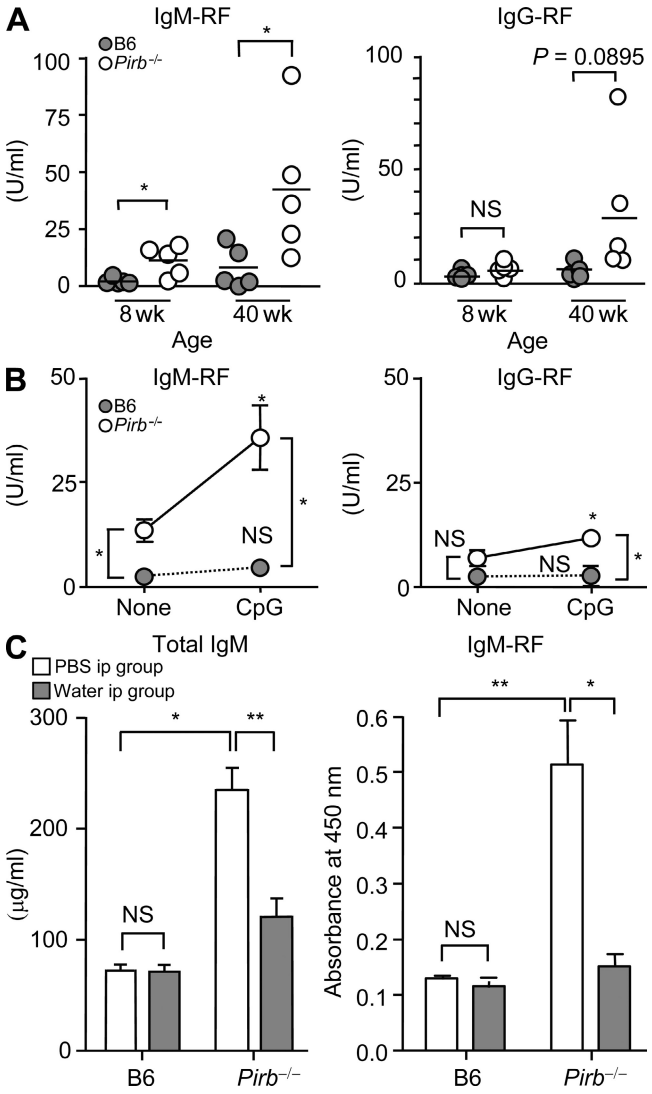

Figure 2. Enhanced RF production in *Pirb*$^{-/-}$ mice. (A) The IgM-RF levels are significantly elevated in *Pirb*$^{-/-}$, aged mice in particular. Sera from wild-type B6 and *Pirb*$^{-/-}$ mice at 8 and 40 wk of age were subjected to measurement of the IgM- and IgG-RF levels by ELISA. Data are shown as means ± SEM (n = 5 mice per group) and are representative of three separate experiments with similar results. Statistical analyses were performed using a Student's t test. *, $P < 0.05$. (B) Both the IgM- and IgG-RF levels in sera were elevated in *Pirb*$^{-/-}$ mice after CpG-B administration into the peritoneum of the animals. B6 and *Pirb*$^{-/-}$ mice at 8 wk of age were injected with 3 nmol CpG-B into the peritoneal cavity. Serum samples collected after 48 and 120 h were analyzed by ELISA for IgM- and IgG-RF, respectively. Data are shown as means ± SEM (n = 4 mice per group) and are representative of three separate experiments with similar results. Statistical analyses were performed using a Student's t test. *, $P < 0.05$. (C) IgM-RF is produced preferentially by peritoneal B cells. B6 and *Pirb*$^{-/-}$ mice at 5 wk of age were injected intraperitoneally with water or PBS as a negative control to achieve relatively specific elimination of the B-1 cells (Murakami et al., 1995). After four rounds of water injection, the total IgM level was significantly decreased and the IgM-RF was substantially lost in sera from *Pirb*$^{-/-}$ mice. Data are shown as means ± SEM (n = 3 mice per group) and are representative of three separate experiments with similar results. Statistical analyses were performed using a Student's t test. *, $P < 0.05$.

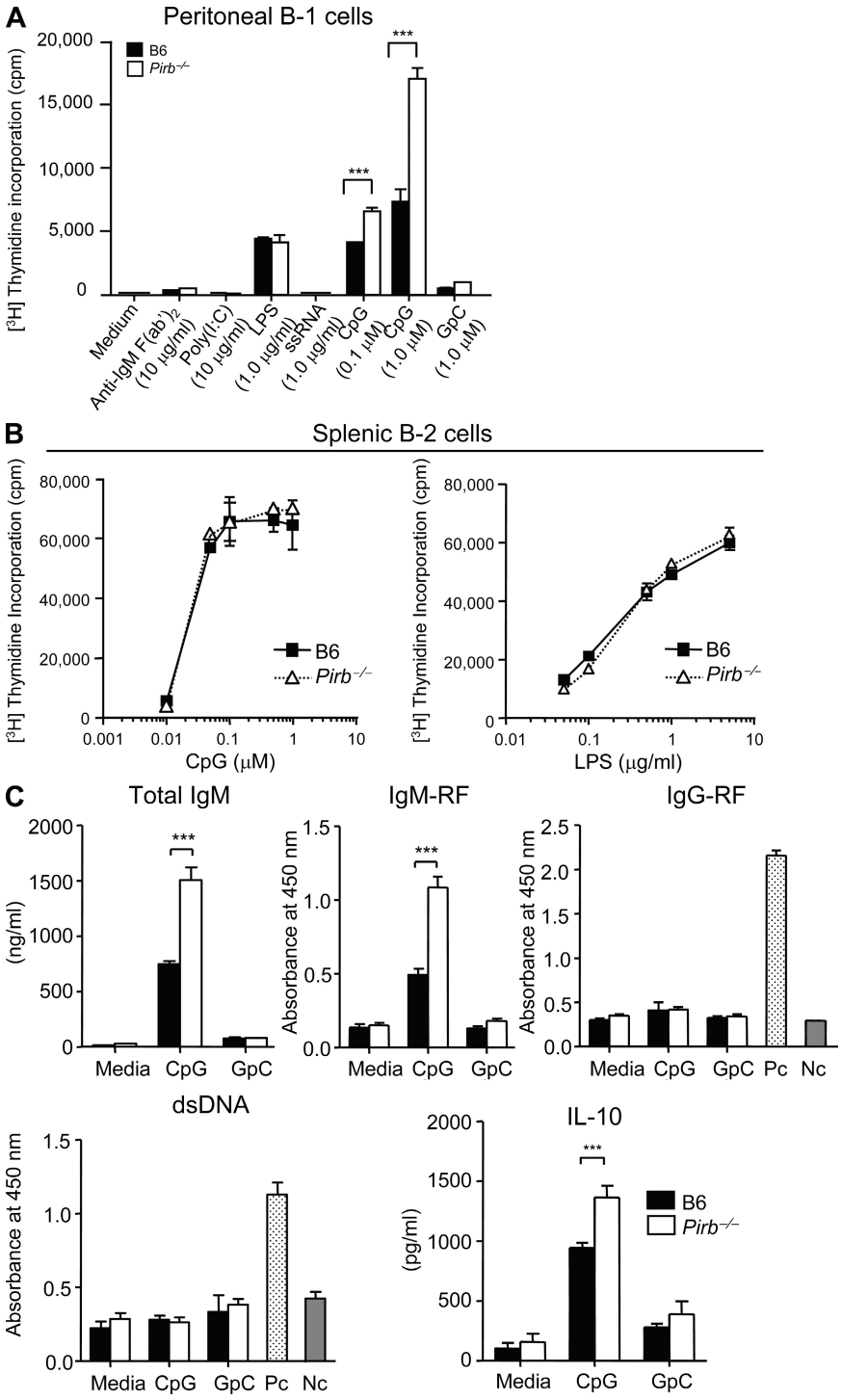

Figure 3. Enhanced responses in peritoneal B-1 cells from *Pirb*$^{-/-}$ mice upon CpG-B stimulation in vitro. (A and B) Proliferation of peritoneal B-1 cells (A) or splenic B-2 cells (B) from wild-type B6 and *Pirb*$^{-/-}$ mice ($n = 5$ per group) with various stimuli. Peritoneal B-1 cells and splenic B-2 cells were pulse labeled with [^{3}H]thymidine during the last 8 h of the 48-h culture period with or without a stimulant. Data are shown as means ± SEM of triplicate cultures and are representative of three independent experiments. Statistical analyses were performed using two-way analysis of variance. ***, $P < 0.001$. (C) Production of Igs, autoantibodies, and a cytokine by peritoneal B-1 cells from B6 and *Pirb*$^{-/-}$ mice ($n = 5$ per group). B-1 cells were stimulated with 1 μM CpG-B or GpC control, and assessed for total IgM, IgM-RF, IgG-RF, anti-dsDNA, and IL-10 by ELISA. Data are shown as means ± SEM of triplicate cultures, and are representative of three independent experiments. Statistical analyses were performed using a Student's *t* test. ***, $P < 0.001$. Provided standard and assay diluent supplemented in the ELISA kit were served as positive control (Pc) and negative control (Nc), respectively.

supernatant was collected after a 20–72-h stimulation of B-1 cells with 1 μM CpG-B, which was subjected to measurement of the contents of autoantibodies and a cytokine by ELISA (Fig. 3 C). We found that total IgM, IgM-RF, and IL-10 release, but not IgG-RF or anti-dsDNA, were significantly more elevated in *Pirb*$^{-/-}$ B-1 cells than in wild-type cells. Collectively, these data indicate that CpG-B stimulation of *Pirb*$^{-/-}$ peritoneal B-1 cells resulted in augmented proliferation, enhanced IgM antibody production (including autoreactive IgM-RF), and IL-10 release in vitro. Although B-1 cells express PIR-B molecules more abundantly on their surface than splenic B-2 cells (Fig. S3 A), the expression of PIR-A, an activating counterpart of PIR-B, is not detected on B-1 cells (Fig. S4, A and B), and the TLR9 level is not augmented in *Pirb*$^{-/-}$ B-1 cells (Fig. S4 C), suggestive of the presence of any PIR-B–mediated inhibitory signaling that specifically regulates TLR9 in B-1 cells.

Augmented phosphorylation of PIR-B and SHP-1 recruitment upon CpG-B stimulation of B-1 cells

Because of the very limited number of purified B-1 cells that we can sort from peritoneal cells, we used whole peritoneal cells or cultured macrophages, which give a grossly similar PIR-B signal upon CpG-B stimulation as B-1 cells (unpublished data), in some analyses of signaling events. PIR-B phosphorylation in peritoneal cells was augmented, reached a maximum as early as 5 min after CpG-B addition, and lasted for at least 20 min (Fig. 4 A). Notably, PIR-B in peritoneal cells in the nonstimulated state was already tyrosine phosphorylated, as in the cases of other cells such as splenic B cells and macrophages (Fig. 4, B and C, B-1 cells and macrophages, respectively; Ho et al., 1999; Kubagawa et al., 1999; Maeda et al., 1999), possibly because of constitutive PIR-B ligation to MHC class I molecules on the same cell surface (Masuda et al., 2007). CpG-B–induced augmentation of PIR-B phosphorylation indeed also occurred in purified B-1 cells 5 min after the stimulation, and was accompanied by a significant increase in SHP-1 recruitment (Fig. 4 B). Importantly, although we also found augmented phosphorylation of PIR-B and enhanced recruitment of SHP-1 upon stimulation of cultured macrophages with CpG-B, but not GpC control DNA (Fig. 4 C, left), these events were not observed in TLR9-deficient cells (Fig. 4 C, right), indicating that CpG-B–mediated PIR-B phosphorylation is dependent

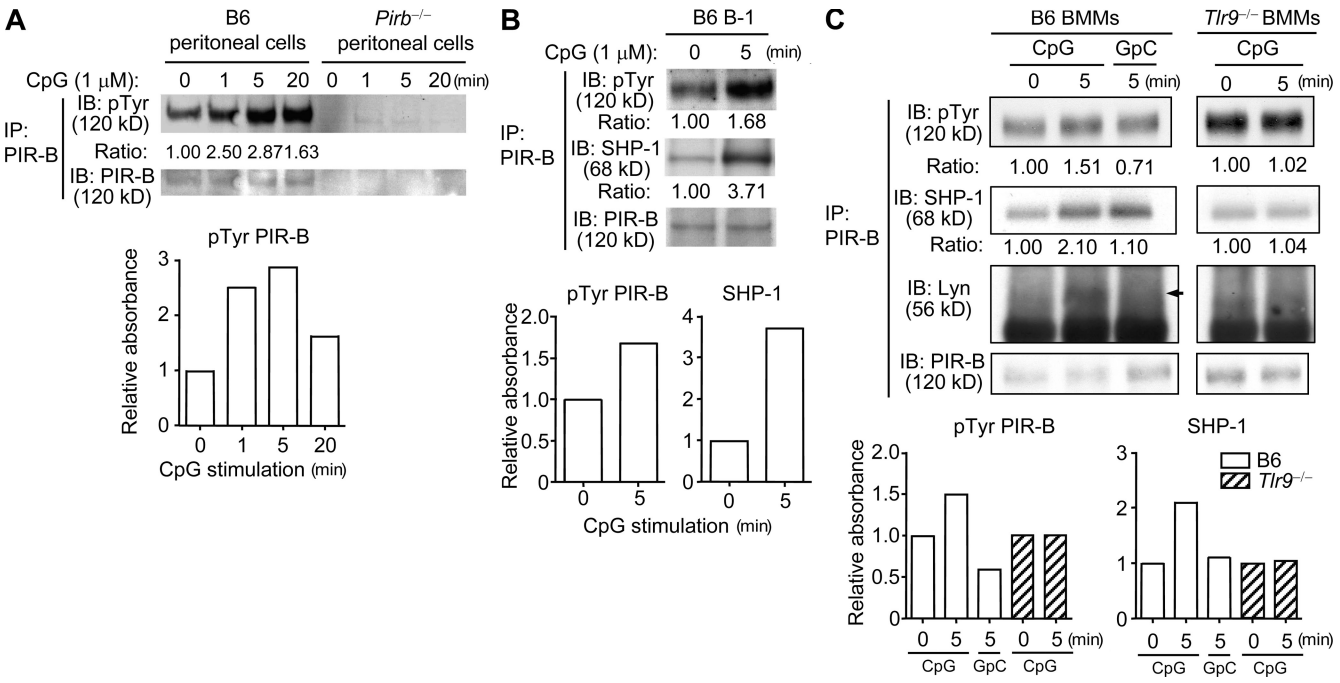

Figure 4. Augmented phosphorylation of PIR-B and enhanced recruitment of SHP-1 in peritoneal B-1 cells stimulated with CpG-B. (A) Time course of tyrosine phosphorylation of PIR-B in peritoneal cells from B6 and *Pirb*$^{-/-}$ mice (n = 8 per group) stimulated with CpG-B. After stimulation with 1 μM CpG-B, samples were taken at various time points and first immunoprecipitated (IP) with anti–PIR-B and then immunoblotted (IB) to visualize PIR-B phosphotyrosine (top), followed by reprobing with anti–PIR-B (bottom). Data are representative of three separate experiments with similar results. (B) Augmented tyrosine phosphorylation of PIR-B and enhanced recruitment of SHP-1 in peritoneal B-1 cells stimulated with CpG-B. B-1 cells from wild-type B6 mice (n = 12) were stimulated with 1 μM CpG-B and subjected to immunoprecipitation and protein blot analysis (IP-Western) to visualize the phosphotyrosylation of PIR-B (top), SHP-1 (middle), and PIR-B (bottom). Data are representative of three separate experiments with similar results. (C) Phosphotyrosylation of PIR-B upon CpG stimulation is dependent on TLR9. Bone marrow–derived cultured macrophages (BMMs) from wild-type B6 mice (left) and TLR9-deficient (*Tlr9*$^{-/-}$) mice (right; n = 4 per group) were stimulated with 1 μM CpG-B or GpC control DNA, and subjected to IP-Western to visualize phosphotyrosylated PIR-B (top), SHP-1 (second from top), Lyn (second from bottom; arrow), and PIR-B (bottom). Data are representative of three separate experiments with similar results. The intensity for each band was estimated by densitometric scanning with normalization as to loading control.

on TLR9. Interestingly, stimulation of macrophages with CpG-B but not GpC induced coprecipitation of PIR-B and Lyn, whereas the stimulation of TLR9-deficient macrophages did not (Fig. 4 C, second from bottom), suggestive of an interaction of Lyn and PIR-B upon TLR9 activation (see following paragraph).

Up-regulated phosphorylation of PIR-B is mediated, at least partly, by Lyn

Preceding studies by others indicated that, in splenic B cells, Lyn is the major Src family kinase that constitutively phosphorylates PIR-B (Ho et al., 1999). To elucidate the molecular mechanisms underlying TLR9-mediated PIR-B phosphorylation, we first examined activation of Lyn in TLR9-sufficient or -deficient B-1 cells stimulated with CpG-B. The phosphorylation level of Lyn was found to be augmented as early as 5 min after CpG-B stimulation of B-1 cells regardless of the presence or absence of PIR-B (Fig. 5, A and B). However, augmented phosphorylation of Lyn was not observed in TLR9-deficient B-1 cells (Fig. 5, C and D). In addition, as noted in the previous paragraph, Lyn–PIR-B coprecipitation was detected in a macrophage lysate prepared after stimulation with CpG-B (Fig. 4 C, second from bottom). These results indicate that Lyn is rapidly activated downstream of TLR9 and strongly suggest that Lyn is a candidate, if not the sole, Src family kinase that phosphorylates PIR-B.

Enhanced activation of NF-κB but not the mitogen-activated protein kinase (MAPK) pathway in PIR-B–deficient B-1 cells after CpG-B stimulation

Next we aimed at elucidating the molecular events occurring in two major downstream cascades of TLR9 activation upon CpG-B stimulation of *Pirb*$^{-/-}$ B-1 cells. Generally, TLR9-mediated signaling leads to activation of NF-κB as well as the MAPK pathway (Akira et al., 2001; Baccala et al., 2007; Krieg and Vollmer, 2007). We observed that the phosphorylation levels of p38 MAPK and Erk were significantly augmented, particularly at 30 min after CpG-B addition, in both wild-type and *Pirb*$^{-/-}$ B-1 cells (Fig. 6, A–C). However, the phosphorylation kinetics and levels were comparable between these cells, suggesting that these phosphorylation events are independent of PIR-B–mediated regulation. Interestingly, however, p65 NF-κB phosphorylation was found to be markedly augmented in *Pirb*$^{-/-}$ B-1 cells as early as 5 min after CpG-B addition (Fig. 6, A and D). These results indicate that the NF-κB p65RelA subunit could be the target molecule located the most downstream of regulation through Lyn-mediated PIR-B phosphorylation, whereas the MAPK pathway is not linked to the PIR-B pathway.

Btk can link the PIR-B pathway and NF-κB cascade

Which molecule acts as an intersection between the PIR-B–SHP-1–initiated inhibitory signaling pathway and the TLR9–NF-κB cascade? Maeda et al. (1999) reported that, in a B cell

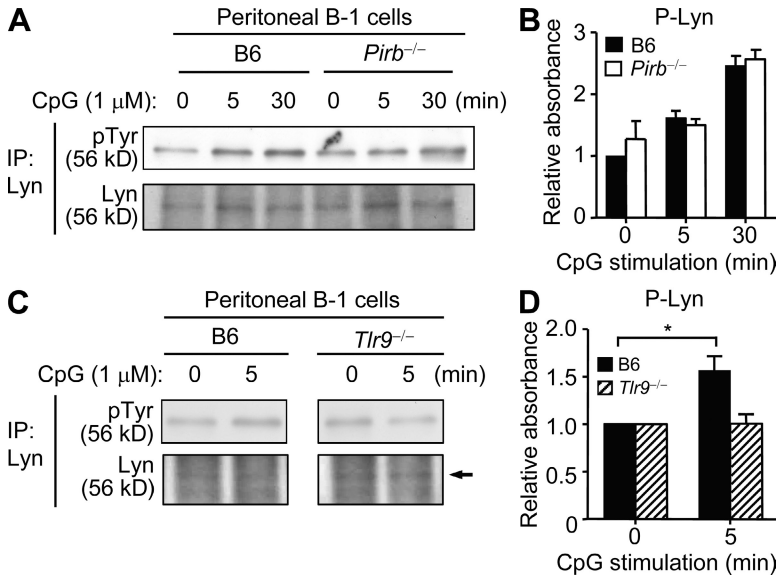

Figure 5. Up-regulated phosphorylation of Lyn upon CpG-B stimulation of wild-type and *Pirb*$^{-/-}$ B-1 cells but not *Tlr9*$^{-/-}$ cells. (A and B) Peritoneal B-1 cells from wild-type B6 and *Pirb*$^{-/-}$ mice (n = 12 per group) were stimulated with 1 μM CpG-B and subjected to IP-Western analysis to visualize the phosphprylated Lyn (A). The phosphorylation levels of Lyn were estimated by densitometric scanning with normalization as to loading control and are depicted as a bar graph (B). Lyn phosphorylation was augmented upon CpG stimulation regardless of the presence or absence of PIR-B. Data are shown as means ± SEM of three separate experiments. (C and D) Peritoneal B-1 cells from wild-type B6 and *Tlr9*$^{-/-}$ mice (n = 12 per group) were stimulated with 1 μM CpG-B and subjected to IP-Western analysis to visualize the phosphorylated Lyn (C). The phosphorylation levels of Lyn were estimated by densitometric scanning with normalization as to loading control and are depicted as a bar graph (D). Augmented Lyn phosphorylation was not observed in *Tlr9*$^{-/-}$ B-1 cells. Data are shown as means ± SEM of three separate experiments. Control bands of Lyn (~56 kD) were obscured by 40–60-kD diffuse bands originated from protein A released from immunoprecipitation beads. *, $P < 0.05$.

line, IIA1.6, Syk, and Btk were the substrates for SHP-1 recruited to PIR-B ITIMs upon stimulation of B cell receptors. This observation prompted us to examine the possible involvement of these two molecules in the TLR9 pathway. Examination of the phosphorylation status of Syk upon CpG-B addition to B-1 cells did not reveal significant enhancement of the phosphorylation in either wild-type or *Pirb*$^{-/-}$ B-1 cells (Fig. 7, A and B), indicating that Syk does not seem to be a critical substrate for SHP-1 recruited to PIR-B ITIMs in B-1 cells. Instead, we found that Btk phosphorylation was markedly augmented 5 min after CpG-B addition in both wild-type and *Pirb*$^{-/-}$ B-1 cells, and the augmentation did not show a marked decrease at least up to 30 min after CpG-B stimulation in *Pirb*$^{-/-}$ B-1 cells (Fig. 7, A and C), indicating that Btk is a major substrate for SHP-1.

Pretreatment of B-1 cells with Src family kinase inhibitors can suppress phosphorylation of Btk and NF-κB p65RelA after CpG-B stimulation

To verify that Lyn could be the most upstream effector for Btk and NF-κB p65RelA phosphorylation, wild-type B-1 cells were pretreated with Src family kinase inhibitors (SU6656 or PP2), stimulated with CpG-B, and examined to determine the phosphorylation levels of Btk and NF-κB p65RelA. We observed that a slight increase in the phosphorylation level of Btk 5 min after CpG-B stimulation was partially blocked by pretreatment with the inhibitors (Fig. 8, A and B). The reduction of the phosphorylation was more evident in the case of NF-κB p65RelA (Fig. 8, A and C). These results indicate that Btk phosphorylation is dependent, at least partly, on an Src family kinase, most likely Lyn, and that NF-κB p65RelA phosphorylation is also a critical event downstream of Src family kinase activation.

DISCUSSION

Recent studies have suggested several feedback regulators for TLR9 activation, including SOCS1 (Rothlin et al., 2007), ATF3 (Whitmore et al., 2007), IRF-4 (Martin et al., 2007), and SHP-1 (An et al., 2008). For example, receptor tyrosine-based activation motif–induced, SOCS1-mediated feedback regulation seems to occur at later stages, such as hours, after TLR9 activation, followed by inflammatory cytokine induction (Rothlin et al., 2007). In contrast, the PIR-B–mediated suppression revealed in this study seems to take place as early as 5 min after CpG-B addition to B-1 cells. Therefore, PIR-B does not seem to fit well into the category of feedback regulatory elements for TLR9. Rather, it plays an important regulatory role in immediate-early cellular responses to TLR9

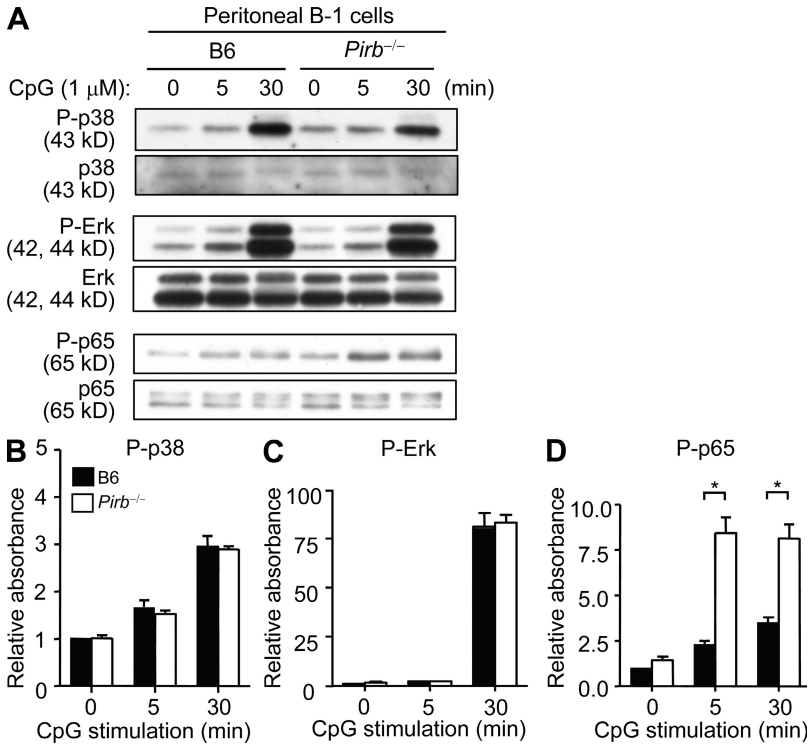

Figure 6. p38 and Erk phosphorylation is not grossly influenced by PIR-B, whereas NF-κB p65RelA phosphorylation is markedly augmented in *Pirb*$^{-/-}$ B-1 cells. (A–D) Immunoblot analysis of phospho-p38, phospho-Erk, and phospho-p65RelA after CpG stimulation of peritoneal B-1 cells from wild-type B6 and *Pirb*$^{-/-}$ mice (n = 10–14 per group). Although the time courses and augmentation magnitudes of the phosphorylation of p38 and Erk were not grossly different between wild-type and *Pirb*$^{-/-}$ B-1 cells (A–C), phosphorylation of NF-κB p65RelA was markedly augmented in *Pirb*$^{-/-}$ B-1 cells (A and D). The intensity for each band was estimated by densitometric scanning with normalization as to loading control. Data are shown as means ± SEM of three separate experiments. *, $P < 0.05$.

activation. PIR-B is constitutively tyrosine phosphorylated at the ITIMs and associates with SHP-1 (Ho et al., 1999; Kubagawa et al., 1999; Maeda et al., 1999), which is critical for maintaining steady-state levels of intracellular phosphotyrosylated proteins. In this study, we found a novel and immediately initiated regulatory circuit for TLR9, namely that PIR-B phosphorylation is immediately augmented by TLR9-initiated Lyn activation, and the concomitant enhancement of SHP-1 recruitment to augmented phospho-ITIMs of PIR-B leads to Btk dephosphorylation, which then attenuates the phosphorylation level of NF-κB p65RelA. The molecular mechanism for the TLR9-initiated Lyn activation, which augments Btk phosphorylation, is currently not known. Interestingly, on the other hand, SHP-1 has recently been demonstrated to be a critical regulator for type I interferon production by macrophages and dendritic cells through inhibition of IRAK1 activation downstream of TLR4 (An et al., 2008), whereas augmented IRAK1 activation is not observed in CpG-B–stimulated *Pirb*$^{-/-}$ B-1 cells (Fig. S5), suggesting that B-1 cells preferentially use Btk as a key intersecting molecule for the inhibitory circuit.

Recent studies have shown that Btk is an important mediator for the TLR9 cascade in addition to MyD88 and TRAF (Doyle et al., 2007; Gilliet et al., 2008). Btk is required for NF-κB activation, participating in the pathway leading to increased phosphorylation of p65RelA activated by TLR8 and TLR9 (Doyle et al., 2007; Lee et al., 2008). As is well known, Btk is a critical kinase for the development and function of B cells, including B-1 cells, by assuring antigen receptor signaling, as has been demonstrated in immunocompromised *Xid* mice and human X-linked agammaglobulinemia, in which Btk is dysfunctional (Bradley et al., 1994; Hashimoto et al., 1996). Our current finding that Btk is a critical link between the TLR9 cascade and the PIR-B–mediated regulatory loop, particularly in B-1 cells expressing abundant PIR-B (Fig. S3 A), provides an insight into the mechanism underlying crosstalk of the innate immune system with ITIM-harboring receptors.

Given that PIR-B might be a negative regulator for TLR9 in B-1 cells, PIR-B–mediated inhibition of TLR9 activation could become potentially harmful for host mammals if their immune system should engage with invading pathogens that otherwise would cause serious infectious diseases. Therefore, it is expected that this regulatory system might be tightly controlled during the course of the capture, sensing,

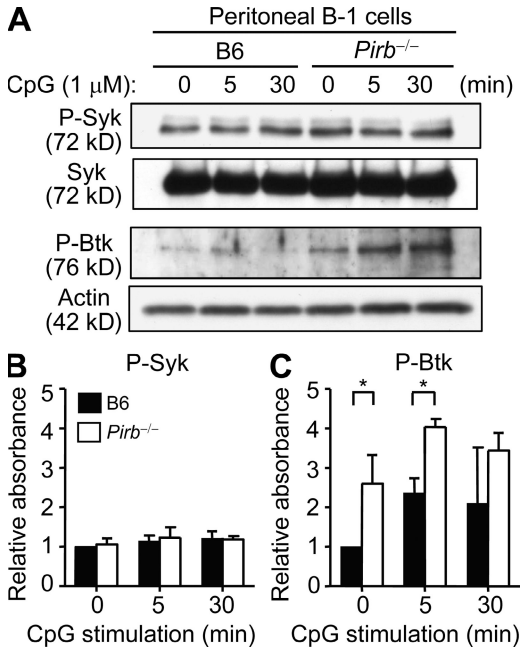

Figure 7. Phosphorylation of Btk but not Syk is markedly up-regulated upon CpG-B stimulation of *Pirb*$^{-/-}$ B-1 cells. (A–C) Peritoneal B-1 cells from B6 and *Pirb*$^{-/-}$ mice (n = 10–14 per group) were stimulated with 1 μM CpG-B and subjected to immunoblot analysis for visualization of phospho-Syk and phospho-Btk (A), which was estimated by densitometric scanning with normalization as to actin (B and C). Data are shown as means ± SEM of three separate experiments. *, $P < 0.05$.

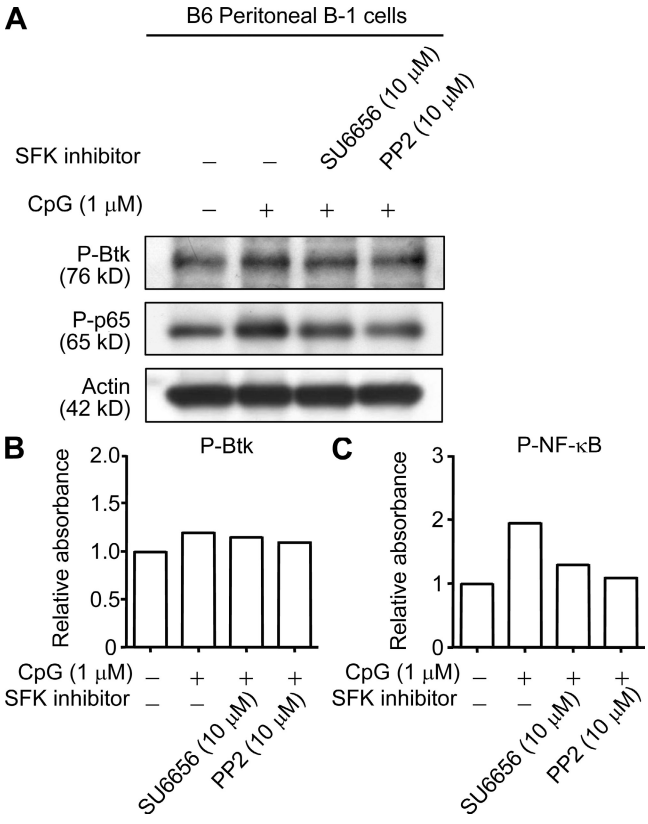

Figure 8. CpG-B–induced phosphorylation of Btk and NF-κB p65RelA in peritoneal B-1 cells is down-regulated by Src family kinase inhibitors. (A–C) Peritoneal B-1 cells from wild-type B6 mice (n = 12) were treated with 10 μM SU6656 or PP2 for 30 min before stimulation with 1 μM CpG-B. 5 min later, cell lysates were subjected to immunoblot analysis to visualize the phosphorylation of Btk (top), NF-κB p65RelA (middle), and loading control β-actin (bottom; A). The phosphorylation levels of Btk and p65RelA were estimated by densitometric scanning with normalization as to actin and are depicted as bar graphs (B and C). Data are representative of three separate experiments with similar results.

processing, and elimination of virulent microbes. How is PIR-B–initiated TLR9 regulation controlled? Although we do not currently have an answer to this question, it is conceivable that cell-surface expression of PIR-B might be down-regulated or the expression of PIR-A with possibly the opposite function, namely the activation of TLR9, might be up-regulated, or both. Another possibility is that spatial communication between PIR-B and TLR9 on, or near, the cell membrane might be uncoupled during serious infections by means of any unknown intracellular mechanism that controls the dynamics of endosomal/lysosomal TLR9 as well as the dynamics of PIR-B. It may be possible that PIR-B on plasma membrane could translocate partially to the endosomal/lysosomal compartment of B-1 cells upon CpG stimulation. Our preliminary confocal laser-scanning microscopic analysis of B-1 cells stimulated with CpG suggests that it could be the case (Fig. S6). Such translocation may account for, at least partly, the reason why endosomal/lysosomal TLR9 can communicate intimately with PIR-B in terms of CpG-initiated, TLR9-mediated signaling and may imply a presence of any uncoupling mechanism for the TLR9–PIR-B communication. On the other hand, although preceding studies have demonstrated the critical roles of inhibition mediated by PIR-B in the maintenance of immune homeostasis (Wheadon et al., 2002; Ujike et al., 2002; Nakamura et al., 2004; Pereira et al., 2004; Zhang et al., 2005; Masuda et al., 2007), the function of the activating counterpart, PIR-A, remains to be determined, but it also can bind to MHC class I molecules (Nakamura et al., 2004). Control mechanisms for balanced, or in some cases unbalanced, PIR-B and PIR-A gene expression are also not known. One notable observation is that PIR-B expression on activated B cells is reduced by IL-4 (Rudge et al., 2002). Another interesting notion is that PIR-A expression on host dendritic cells is significantly augmented during the induction phase of experimental acute graft-versus-disease induced in *Pirb*$^{-/-}$ mice (Nakamura et al., 2004). Obviously, we need more precise knowledge on the regulation of PIR-A and PIR-B, and the spatial communication between membrane PIR-B and endosomal/lysosomal TLR9.

CD5$^+$ B-1 cells are considered to be involved in some autoimmune diseases in which RF is frequently detected or RF production is directly coupled to the disease (Hardy et al., 1987; Sowden et al., 1987; Youinou et al., 1990). Also, RF$^+$ B cells are effectively activated via the IgG2a–chromatin immune complex and synergistic stimulation of TLR9-mediated signaling (Leadbetter et al., 2002). It is known that RF can bind to anti-dsDNA autoantibodies and can form immune complexes (Izui and Eisenberg, 1980). Also, it has been reported that RF itself has cryoglobulin activity and causes glomerulonephritis without any other additional factors (Gyotoku et al., 1987). Our observations on glomerulonephritis in *Pirb*$^{-/-}$*Fas*^{lpr} mice with markedly and specifically elevated IgM- and IgG-RF productions, but not other autoantibodies examined, suggest that IgM- and IgG-RF autoantibodies, namely anti-IgG Fc antibodies, are factors that worsen the disease, presumably by accelerating the deposition of IgG autoantibodies against basement membranes of glomeruli. Considering these observations, it may increasingly become important to manipulate the PIR-B–mediated inhibitory system in the regulation of autoimmune diseases while maintaining the integrity of TLR9-mediated microbial sensing, in such cases as rheumatoid arthritis (Newkirk, 2002). Understanding of the PIR-B system in B-1 cells may lead to the development of novel and effective ways toward controlling autoimmune diseases.

MATERIALS AND METHODS

Mice. C57BL/6 (B6) mice were purchased from Charles River Laboratories. *Pirb*$^{-/-}$ mice were generated (Ujike et al., 2002) and backcrossed with B6 mice for 12 generations. *Pirb*$^{-/-}$*Fas*^{lpr} mice were generated by crossing B6.*Fas*^{lpr} mice (C57BL/6J Jms Slc-*lpr/lpr*; The Jackson Laboratory) with B6.*Pirb*$^{-/-}$ mice and by intercrossing between the littermates. TLR9-deficient (*Tlr9*$^{-/-}$) mice were purchased from Oriental BioService, Inc. Mice were maintained and bred in the Animal Facility of the Institute of Development, Aging, and Cancer, Tohoku University, an environmentally controlled and specific pathogen-free facility, according to guidelines for experimental animals defined by the university, and animal protocols were reviewed and approved by the Animal Studies Committee of the university. All experiments were performed on 6–50-wk-old age-matched male and female mice.

Reagents and antibodies. LPS (B8) was purchased from Sigma-Aldrich. Poly(I:C) and ssRNA/LyoVec were obtained from InvivoGen. Anti-IgM F(ab′)$_2$ was purchased from Invitrogen. Phosphothioate–CpG-B oligodeoxynucleotide (ODN1826; 5′-TCCATGACGTTCCTGACGTT-3′) and phosphothioate-GpC (5′-TCCATGAGCTTCCTGAGCTT-3′) were synthesized by Hokkaido System Science Co., Ltd. Src kinase inhibitors SU6656 and PP2 were obtained from EMD. Antibodies to phospho-Syk (Tyr352), Syk, Lyn, phospho–p44/42 MAPK (Thr202/Tyr204 and D13.14.4E), phospho-p38 (Thr180/Tyr182), p38 (5F11), phospho–NF-kB p65 (Ser536), and NF-κB p65 were obtained from Cell Signaling Technology. Phospho-Btk (Tyr550) antibody was obtained from Abcam. Antibodies to Btk, Erk, PIR-B (p91), anti-IRAK1, anti–mouse monoclonal Btk (E-9), and SHP-1 were purchased from Santa Cruz Biotechnology, Inc. The horseradish peroxidase (HRP)–conjugated antiphosphotyrosine mAb (RC20) was purchased from BD. The antibody to β-actin was obtained from Sigma-Aldrich.

Cell separation. For separation of splenic B cells, B220$^+$ cells were purified with a magnetic-activated cell sorter (MACS; Miltenyi Biotec). For preparation of peritoneal B-1 cells, peritoneal cells were isolated by washing of the peritoneal cavity with ice-cold RPMI 1640 containing 10% FCS. Peritoneal cells were first blocked with anti–mouse FcγR mAb (2.4G2; BD) and then stained with allophycocyanin (APC)-labeled anti-B220 (RA3-6B2; BD) and FITC-labeled anti-CD11b (M1/70; BD) mAbs, and B220$^+$CD11b$^+$ cells were sorted using a FACSAria (BD). The purity of the sorted populations was consistently >95%, as determined by the B220$^+$CD11b$^+$ phenotype. Bone marrow cells from femurs were cultured in α-MEM containing 10% FCS and 20 ng/ml M-CSF (PeproTech) at 37°C. After 7 d, the adherent cells were used as bone marrow–derived macrophages (BMMs).

Proliferation assay. 10^5 splenic B cells per well and 2.5×10^4 peritoneal B-1 cells per well were cultured in 96-well flat plates (Corning) with RPMI 1640 containing 10% FCS, 1 mM sodium pyruvate, and supplemented antibiotics. The cells were activated with the reagents described in Reagents and antibodies. After 48 h of stimulation, proliferation was determined as [^{3}H]thymidine uptake.

Measurement of antibodies and a cytokine. 5×10^4 peritoneal B-1 cells per well were cultured in 96-well flat plates with or without stimulants. The supernatants of 20–72-h-cultured peritoneal B-1 cells were collected, and the amounts of anti-dsDNA antibodies, RF, IgM, and IL-10 were determined

with mouse anti-dsDNA and anti-ssDNA ELISA kits (Shibayagi Co.), mouse IgM and IgG RF ELISA kits (Shibayagi), a mouse IgM ELISA quantification kit (Bethyl Laboratories, Inc.), and a mouse IL-10 ELISA MAX (BioLegend). Serum from aged mice was collected, and the amounts of anti-dsDNA antibodies, total IgM, and RF were determined by ELISA as described. The amount of anti-SS-B/La antibodies was determined with a mouse anti-SSB/La antibodies ELISA kit (Alpha Diagnostic Intl. Inc.).

Immunoprecipitation analysis. Peritoneal cells, peritoneal B-1 cells, and BMMs were incubated for 0, 5, or 30 min at 37°C with 1 μM CpG-B. Cells were solubilized in a lysis buffer (0.75% Briji-97, 50 mM Hepes [pH 7.4], 100 mM NaCl, and 10% glycerol) containing 2 mM sodium vanadate and supplemented with protease inhibitors. Cell lysates were incubated with Dynabeads protein A (Invitrogen) preincubated with anti–mouse PIR-B (p91; Santa Cruz Biotechnology, Inc.) or anti-Lyn (Cell Signaling Technology). The immunoprecipitates were separated in an SDS-PAGE gel, transferred to a polyvinylidene difluoride (PVDF) membrane (Millipore), and detected with the HRP-antiphosphotyrosine mAb (RC20; BD), anti–SH-PTP-1 (Santa Cruz Biotecnology, Inc.), and HRP-labeled goat anti–rabbit IgG (Cell Signaling Technology) using an enhanced chemiluminescence system (GE Healthcare). The membranes were stripped off with a stripping buffer comprising 62.5 mM Tris (pH 6.8), 100 mM 2-ME, and 2% SDS, and reprobed with anti-p91 or anti-Lyn and HRP–rabbit anti–goat IgG (Millipore) or TrueBlot anti–rabbit IgG HRP (eBioscience).

Immunoblot analysis. Peritoneal B-1 cells were solubilized in a lysis buffer (1% NP-40, 20 mM Tris [pH 7.3], 150 mM NaCl, 10 mM EDTA, and 10% glycerol) containing 2 mM sodium vanadate and 50 mM sodium fluoride, and supplemented with protease inhibitors. Cell lysates were separated by SDS-PAGE and transferred to a PVDF membrane, followed by detection with the appropriate antibodies. Signal intensities of each protein were estimated by densitometric scanning (Dolphin View band tool; KURABO).

Flow cytometry. For flow cytometric analysis, the following mAbs obtained from BD were used: purified FITC-, PE-, APC-, or biotin-conjugated antibodies against mouse B220 (RA3-6B2), IgM (R6-60.2), IgD (11-26), CD3 (145-2C11), CD5 (Ly-1), CD11b (M1/70), and CD138 (281-2); rat IgG1 (A101-1); rat IgG2a (R35-95); PECy5-conjugated streptavidin; APC-conjugated streptavidin; and anti–mouse FcγR (2.4G2). For PIR-B staining, peritoneal cells or splenocytes were stained with anti–PIR-A/B (6C1; BD). After washing, the cells were stained with PE-conjugated goat anti–rat IgG $F(ab')_2$ antibody (AbD Serotec). After washing, the cells were stained with the appropriate antibodies for the surface antigens of B cells. For intracellular TLR9 or Btk staining, peritoneal cells or splenocytes were fixed with Cytofix/Cytoperm (BD). After cells had been washed in a permeabilization buffer (Perm/Wash; BD), they were stained with biotin-conjugated anti–mouse TLR9 (M9.D6; eBioscience) and APC-conjugated streptavidin or rabbit anti–mouse Btk antibody (M-138; Santa Cruz Biotechnology Inc.) and Alexa Fluor 647–conjugated goat anti–rabbit IgG (Invitrogen). Cell surfaces were stained by standard techniques, and flow cytometry was performed with a FACSCalibur (BD) and analyzed with FlowJo software (Tree Star, Inc.).

Reduction of peritoneal B cells. For peritoneal B cell reduction in mice, we used the method described by Murakami et al. (1995). In brief, distilled water or PBS, as a negative control, was injected every week into the peritoneal cavity of mice. The doses of injected water and PBS depended on the size of the mice as follows: 1 ml for 4–8 wk of age or 2 ml for 8 wk of age and older. Blood was collected after the fourth injection of water or PBS.

Histological study and immunohistochemistry. Kidney samples and foot joints were fixed with 4% neutral-buffered formalin-PBS, embedded in paraffin, sectioned at 2 μm, and stained with PAS or hematoxylin and eosin. To assay for immune complex deposition, formalin-fixed and paraffin-embedded kidney sections were deparaffinized in xylene and dehydrated through a graded ethanol series. After washing with distilled water, sections were incubated with trypsin (Nichirei) for 50 min at 37°C and washed three times with PBS. Sections were incubated with Alexa Fluor 488–conjugated anti–mouse IgG, IgM (Invitrogen), goat IgG fraction to mouse complement C3 (Cappel; MP Biomedicals), or Alexa Fluor 488–conjugated anti–goat IgG (Invitrogen). To detect antinuclear antibodies in sera, HEp2 cell plates (FLUORO HEPANA test; MBL International) were stained with sera from B6 *Pirb*$^{-/-}$, *Fas*^{lpr}, *Pirb*$^{-/-}$*Fas*^{lpr}, and *Fcgr2b*$^{-/-}$*Fas*^{lpr} (Yajima et al., 2003) mice at different dilutions, and detected with FITC-conjugated anti–mouse IgG (Cappel; MP Biomedicals). Samples were examined under microscopes (BX50 [Olympus] and VB-7000 [Keyence]).

Renal function test. Serum from mice of each strain at 40 wk of age was collected, and the amounts of blood urea nitrogen and creatinine were determined with a dry chemistry analyzer (Fujifilm).

Confocal laser-scanning microscopic analysis. MACS-sorted peritoneal B-1 cells ($CD3^-$, $F4/80^-$, $CD23^-$, and IgM^+) from B6 mice were cultured with Cy5-conjugated CpG-B (ODN1826; Nihon Gene Research Laboratories Inc.) and LysoTracker Green DND-26 (Invitrogen) for 30 min. After fixation with Cytofix/Cytoperm, cells were permeabilized with Perm/Wash and stained with biotin-conjugated anti–mouse PIR-A/B (6C1) or rat IgG1 isotype control (BD) and Alexa Fluor 546–conjugated streptavidin (Invitrogen). Samples were examined under a microscope (Fluoview FV1000; Olympus).

Statistical analysis. Statistical analyses were performed using two-way analysis of variance or Student's *t* test. $P < 0.05$ is considered as statistically significant.

Online supplemental material. Fig. S1 presents additional data showing that PIR-B deletion leads to renal dysfunction when combined with the *Fas*^{lpr} mutation but does not have an impact on arthritis development, or antinuclear, anti–SS-B/La, and anti–β2-GPI autoantibody production. Fig. S2 shows diminishment of peritoneal B cells in *Pirb*$^{-/-}$ mice by repeated water injection. Fig. S3 shows that peritoneal B-1 cells express much more PIR-B than splenic B-2 cells, that TLR9 expression does not differ between B-1 and B-2 cells, and that Btk expression is higher in B-1 than B-2 cells. Fig. S4 shows that PIR-A expression is not detected on B-1 cells and that TLR9 expression does not change. Fig. S5 shows that the IRAK1 degradation level was not significantly altered in PIR-B–deficient B-1 cells. Fig. S6 shows that PIR-B can translocate into the endolysosomal compartment after CpG-B stimulation of B-1 cells. Table S1 presents hematocrit values for *Pirb*$^{-/-}$ and *Pirb*$^{-/-}$*Fas*^{lpr} mice. Online supplemental material is available at http://www.jem.org/cgi/content/full/jem.20082392/DC1.

We thank N. Halewood for editorial assistance, and Y. Ito and A. Sugahara-Tobinai for the outstanding technical support.

This work was supported in part by the Core Research for Evolutional Science and Technology Program of the Japan Science and Technology Agency, a Grant-in-Aid from the Ministry of Education, Culture, Sports, Science, and Technology of Japan, the Kanae Foundation for the Promotion of Medical Science, and a grant from the 21st Century Center of Excellence (COE) Program for Innovative Therapeutic Development Toward the Conquest of Signal Transduction Diseases and the Global COE Program for Network Medicine.

The authors have no conflicting financial interest.

Submitted: 23 October 2008
Accepted: 28 July 2009

REFERENCES

Akira, S., K. Takeda, and T. Kaisho. 2001. Toll-like receptors: critical proteins linking innate and acquired immunity. *Nat. Immunol.* 2:675–680.

An, H., J. Hou, J. Zhou, W. Zhao, H. Xu, Y. Zheng, Y. Yu, S. Liu, and X. Cao. 2008. Phosphatase SHP-1 promotes TLR- and RIG-I-activated production of type I interferon by inhibiting the kinase IRAK1. *Nat. Immunol.* 9:542–550.

Baccala, R., K. Hoebe, D.H. Kono, B. Beutler, and A.N. Theofilopoulos. 2007. TLR-dependent and TLR-independent pathways of type I interferon induction in systemic autoimmunity. *Nat. Med.* 13:543–551.

Baumgarth, N., J.W. Tung, and L.A. Herzenberg. 2005. B-1 B cells: development, selection, natural autoantibody and leukemia. *Springer Semin. Immunopathol.* 26:347–362.

Berland, R., and H.H. Wortis. 2002. Origins and functions of B-1 cells with notes on the role of CD5. *Annu. Rev. Immunol.* 20:253–300.

Bradley, L.A., A.K. Sweatman, R.C. Lovering, A.M. Jones, G. Morgan, R.J. Levinsky, and C. Kinnon. 1994. Mutation detection in the X-linked agammaglobulinemia gene, BTK, using single strand conformation polymorphism analysis. *Hum. Mol. Genet.* 3:79–83.

Carroll, M.C., and V.M. Holers. 2005. Innate autoimmunity. *Adv. Immunol.* 86:137–157.

De Re, V., S. De Vita, D. Sansonno, D. Gasparotto, M.P. Simula, F.A. Tucci, A. Marzotto, M. Fabris, A. Gloghini, A. Carbone, et al. 2006. Type II mixed cryoglobulinaemia as an oligo rather than a mono B-cell disorder: evidence from GeneScan and MALDI-TOF analyses. *Rheumatology (Oxford).* 45:685–693.

Doyle, S.L., C.A. Jefferies, C. Feighery, and L.A.J. O'Neill. 2007. Signaling by Toll-like receptors 8 and 9 requires Bruton's tyrosine kinase. *J. Biol. Chem.* 282:36953–36960.

Genestier, L., M. Taillardet, P. Mondiere, H. Gheit, C. Bella, and T. Defrance. 2007. TLR agonists selectively promote terminal plasma cell differentiation of B cell subsets specialized in thymus-independent responses. *J. Immunol.* 178:7779–7786.

Gilliet, M., W. Cao, and Y.J. Liu. 2008. Plasmacytoid dendritic cells: sensing nucleic acids in viral infection and autoimmune diseases. *Nat. Rev. Immunol.* 8:594–606.

Groom, J.R., C.A. Fletcher, S.N. Walters, S.T. Grey, S.V. Watt, M.J. Sweet, M.J. Smyth, C.R. Mackay, and F. Mackay. 2007. BAFF and MyD88 signals promote a lupuslike disease independent of T cells. *J. Exp. Med.* 204:1959–1971.

Gururajan, M., J. Jacob, and B. Pulendran. 2007. Toll-like receptor expression and responsiveness of distinct murine splenic and mucosal B-cell subsets. *PLoS One.* 2:e863.

Gyotoku, Y., M. Abdelmoula, F. Spertini, S. Izui, and P.H. Lambert. 1987. Cryoglobulinemia induced by monoclonal immunoglobulin G rheumatoid factors derived from autoimmune MRL/MpJ-*lpr/lpr* mice. *J. Immunol.* 138:3785–3792.

Hardy, R.R., K. Hayakawa, M. Shimizu, K. Yamasaki, and T. Kishimoto. 1987. Rheumatoid factor secretion from human Leu-1$^+$ B cells. *Science.* 236:81–83.

Hashimoto, S., S. Tsukada, M. Matsushita, T. Miyawaki, Y. Niida, A. Yachie, S. Kobayashi, T. Iwata, H. Hayakawa, H. Matsuoka, et al. 1996. Identification of Bruton's tyrosine kinase (Btk) gene mutations and characterization of the derived proteins in 35 X-linked agammaglobulinemia families: a nationwide study of Btk deficiency in Japan. *Blood.* 88:561–573.

Hayami, K., D. Fukuta, Y. Nishikawa, Y. Yamashita, M. Inui, Y. Ohyama, M. Hikida, H. Ohmori, and T. Takai. 1997. Molecular cloning of a novel murine cell-surface glycoprotein homologous to killer cell inhibitory receptors. *J. Biol. Chem.* 272:7320–7327.

Ho, L.H., T. Uehara, C.C. Chen, H. Kubagawa, and M.D. Cooper. 1999. Constitutive tyrosine phosphorylation of the inhibitory paired Ig-like receptor PIR-B. *Proc. Natl. Acad. Sci. USA.* 96:15086–15090.

Iwasaki, A., and R. Medzhitov. 2004. Toll-like receptor control of the adaptive immune responses. *Nat. Immunol.* 5:987–995.

Izui, S., and R.A. Eisenberg. 1980. Circulating anti-DNA-rheumatoid factor complexes in MRL/1 mice. *Clin. Immunol. Immunopathol.* 15:536–551.

Krieg, A.M., and J. Vollmer. 2007. Toll-like receptors 7, 8, and 9: linking innate immunity to autoimmunity. *Immunol. Rev.* 220:251–269.

Kubagawa, H., P.D. Burrows, and M.D. Cooper. 1997. A novel pair of immunoglobulin-like receptors expressed by B cells and myeloid cells. *Proc. Natl. Acad. Sci. USA.* 94:5261–5266.

Kubagawa, H., C.C. Chen, L.H. Ho, T.S. Shimada, L. Gartland, C. Mashburn, T. Uehara, J.V. Ravetch, and M.D. Cooper. 1999. Biochemical nature and cellular distribution of the paired immunoglobulin-like receptors, PIR-A and PIR-B. *J. Exp. Med.* 189:309–318.

Leadbetter, E.A., I.R. Rifkin, A.M. Hohlbaum, B.C. Beaudette, M.J. Shlomchik, and A. Marshak-Rothstein. 2002. Chromatin-IgG complexes activate B cells by dual engagement of IgM and Toll-like receptors. *Nature.* 416:603–607.

Lee, K.G., S. Xu, E.T. Wong, V. Tergaonkar, and K.P. Lam. 2008. Bruton's tyrosine kinase separately regulates NFkappaB p65RelA activation and cytokine interleukin (IL)-10/IL-12 production in TLR9-stimulated B Cells. *J. Biol. Chem.* 283:11189–11198.

Maeda, A., A.M. Scharenberg, S. Tsukada, J.B. Bolen, J.-P. Kinet, and T. Kurosaki. 1999. Paired immunoglobulin-like receptor B (PIR-B) inhibits BCR-induced activation of Syk and Btk by SHP-1. *Oncogene.* 18:2291–2297.

Marsland, B.J., and M. Kopf. 2007. Toll-like receptors: paving the path to T cell-driven autoimmunity? *Curr. Opin. Immunol.* 19:611–614.

Martin, H.J., J.M. Lee, D. Walls, and S.D. Hayward. 2007. Manipulation of the toll-like receptor 7 signaling pathway by Epstein-Barr virus. *J. Virol.* 81:9748–9758.

Masuda, A., A. Nakamura, T. Maeda, Y. Sakamoto, and T. Takai. 2007. Cis binding between inhibitory receptors and MHC class I can regulate mast cell activation. *J. Exp. Med.* 204:907–920.

Montecino-Rodriguez, E., and K. Dorshkind. 2006. New perspectives in B-1 B cell development and function. *Trends Immunol.* 27:428–433.

Murakami, M., H. Yoshioka, T. Shirai, T. Tsubata, and T. Honjo. 1995. Prevention of autoimmune symptoms in autoimmune-prone mice by elimination of B-1 cells. *Int. Immunol.* 7:877–882.

Nakamura, A., E. Kobayashi, and T. Takai. 2004. Exacerbated graft-versus-host disease in Pirb−/− mice. *Nat. Immunol.* 5:623–629.

Newkirk, M.M. 2002. Rheumatoid factors: host resistance or autoimmunity? *Clin. Immunol.* 104:1–13.

Ochsenbein, A.F., T. Fehr, C. Lutz, M. Suter, F. Brombacher, H. Hengartner, and R.M. Zinkernagel. 1999. Control of early viral and bacterial distribution and disease by natural antibodies. *Science.* 286:2156–2159.

Pereira, S., H. Zhang, T. Takai, and C.A. Lowell. 2004. The inhibitory receptor PIR-B negatively regulates neutrophil and macrophage integrin signaling. *J. Immunol.* 173:5757–5765.

Rothlin, C.V., S. Ghosh, E.I. Zuniga, M.B. Oldstone, and G. Lemke. 2007. TAM receptors are pleiotropic inhibitors of the innate immune response. *Cell.* 131:1124–1136.

Rudge, E.U., A.J. Cutler, N.R. Pritchard, and K.G. Smith. 2002. Interleukin 4 reduces expression of inhibitory receptors on B cells and abolishes CD22 and FcγRII-mediated B cell suppression. *J. Exp. Med.* 195:1079–1085.

Sowden, J.A., P.J. Roberts-Thomson, and H. Zola. 1987. Evaluation of CD5-positive B cells in blood and synovial fluid of patients with rheumatic diseases. *Rheumatol. Int.* 7:255–259.

Tung, J.W., and L.A. Herzenberg. 2007. Unraveling B-1 progenitors. *Curr. Opin. Immunol.* 19:150–155.

Ujike, A., K. Takeda, A. Nakamura, S. Ebihara, K. Akiyama, and T. Takai. 2002. Impaired dendritic cell maturation and increased T(H)2 responses in PIR-B(−/−) mice. *Nat. Immunol.* 3:542–548.

Wheadon, H., N.R. Paling, and M.J. Welham. 2002. Molecular interactions of SHP1 and SHP2 in IL-3-signalling. *Cell. Signal.* 14:219–229.

Whitmore, M.M., A. Iparraguirre, L. Kubelka, W. Weninger, T. Hai, and B.R. Williams. 2007. Negative regulation of TLR-signaling pathways by activating transcription factor-3. *J. Immunol.* 179:3622–3630.

Yajima, K., A. Nakamura, A. Sugahara, and T. Takai. 2003. FcgammaRIIB deficiency with Fas mutation is sufficient for the development of systemic autoimmune disease. *Eur. J. Immunol.* 33:1020–1029.

Youinou, P., L. Mackenzie, P. Katsikis, G. Merdrignac, D.A. Isenberg, N. Tuaillon, A. Lamour, P. Le Goff, J. Jouquan, A. Drogou, et al. 1990. The relationship between CD5-expressing B lymphocytes and serologic abnormalities in rheumatoid arthritis patients and their relatives. *Arthritis Rheum.* 33:339–348.

Zhang, H., F. Meng, C.L. Chu, T. Takai, and C.A. Lowell. 2005. The Src family kinases Hck and Fgr negatively regulate neutrophil and dendritic cell chemokine signaling via PIR-B. *Immunity.* 22:235–246.